Statetostate photodissociation of the fundamental symmetric stretch vibration of water prepared by stimulated Raman excitation

D. David, A. Strugano, I. Bar, and S. Rosenwaks

Citation: The Journal of Chemical Physics **98**, 409 (1993); doi: 10.1063/1.464634
View online: http://dx.doi.org/10.1063/1.464634
View Table of Contents: http://scitation.aip.org/content/aip/journal/jcp/98/1?ver=pdfcov
Published by the AIP Publishing

State-to-state photodissociation of the fundamental symmetric stretch vibration of water prepared by stimulated Raman excitation

D. David, A. Strugano, I. Bar, and S. Rosenwaks
Department of Physics, Ben-Gurion University of the Negev, Beer-Sheva 84105, Israel

(Received 17 August 1992; accepted 22 September 1992)

The state-to-state photodissociation at 193 nm of the fundamental symmetric stretch vibration of water, H_2O (1,0,0), is studied. Stimulated Raman excitation and coherent anti-Stokes Raman scattering are used to prepare and detect, respectively, particular rotational states of H_2O (1,0,0). Laser induced fluorescence is used for monitoring the OH species which are formed from particularly selected rotational states of the H_2O (1,0,0) and also from photodissociation of all occupied rotational states of the ground vibrational state, H_2O (0,0,0), at room temperature. The cross section for photodissociation from a particular rotation of H_2O (1,0,0) at 193 nm is found to be $\sim$550 times greater than that for H_2O (0,0,0). The formation of the OH product in different rotational, Λ-doublet and spin–orbit states is analyzed for the photodissociation of H_2O (0,0,0) and for the photodissociation of the 1_{01}, $1_{10}+1_{11}$, $2_{12}+2_{11}$, and 3_{03} rotational states of H_2O (1,0,0). The rotational distribution of the OH resulting from photodissociation of H_2O (1,0,0) shows a structured distribution that is dependent on the particular rotation of the vibrationally excited state, while that resulting from photodissociation of H_2O (0,0,0) presents a smooth distribution. The Λ-doublet ratio in the two spin–orbit states shows preference of the A'' component for photodissociation from the above rotational states of H_2O (1,0,0), while only a small preference at high N is observed for photodissociation from the ground vibrational state. The results are compared to available theoretical calculations based on the Franck–Condon model and show reasonable agreement between experiment and theory.

I. INTRODUCTION

Triatomic molecules are particularly appealing objects for both theoretical and experimental studies of photodissociation. This is because they are small enough to allow *ab initio* calculations of potential surfaces and photodynamics and yet retain the complexity of different vibrational degrees of freedom. However, quantitative comparison with theory requires experiments that prepare reactant molecules in specific initial states to avoid the averaging over different quantum states. Also, it is necessary to determine accurately the populations in the various final quantum states of the photofragments.

The water molecule is theoretically tractable and is an ideal candidate for *state-to-state* photodissociation experiments. Its large rotational constants allow selective excitation in particular states from a room temperature sample. Its promotion to the $A(^1B_1)$ state continuum, which is a well defined electronic state that is separated from the next two singlet states [$B(^1A_1)$ and $C(^1B_1)$], with a photolysis wavelength at the far end of the absorption spectrum, generates only ground electronic state fragments OH ($X\,^2\Pi$) +H (^2S).[1] The resulting OH fragment is detected via laser induced fluorescence (LIF) and the population in the various final quantum states can be easily determined.

The experimental and theoretical investigations in the first absorption band have been recently reviewed by Engel *et al.*[2] and earlier by Andresen and Schinke.[3] The theoretical studies of Schinke and co-workers[4] mostly make use of the semiempirical ground-state potential energy surface (PES) of Sorbie and Murrell[5] and of the *ab initio* PES of the purely repulsive $A(^1B_1)$ state of Steammler and Palma.[6] These studies are carried out in order to obtain state-to-state cross sections and absorption spectra for the photolysis of water isotopomers, and to predict the dependence of the vibrational excitation of the OH product on the photolysis wavelength.[4] The calculated spectrum consists of a broad continuum with a maximum around 165 nm and perfectly reproduces the measured spectrum.[7] Until recently, measurements of vibrational-state distributions were available for the photolysis wavelengths of 157 and 193 nm,[8–10] showing a very good agreement with theory. Using LIF to probe the OH fragments obtained from photolysis at 157 nm, population ratio of 1:1:0.58 [corrected for predissociation of OH ($A\,^2\Sigma^+$)] was obtained for the three vibrational levels 0, 1, and 2, respectively.[3] Very recently, Mikulecki *et al.*[11] reconsidered the 157 nm photolysis and also photolyzed water via two photon excitation at 354.6 nm (corresponding to 177.3 nm). They measured the complete vibrational distribution for 157 nm photodissociation by using nondiagonal pumping to probe also the higher vibrational states of OH (up to $v''=5$) and obtained a value of 1.8 for the population ratio between the 0 and 1 vibrational states. These results disagree with the calculations[4] as well as with the earlier measurements of Andresen *et al.*[3,8] Furthermore, the observed lack of vibrational excitation for the 177.3 nm photolyis carried out by Mikulecki *et al.*[11] and independently in our laboratory[12] disagree with the theoretical studies[2–4] that predicted population up to $v''=2$, where $\sim$5% of the population is in $v''=1$ for photolysis at 179.7 nm.

In addition, the general Franck–Condon (FC) theory

of Balint-Kurti[13] has been applied to water[9,14] and the results were compared to the distributions measured by Hausler *et al.*[9] for 193 nm photolysis of the asymmetric stretch vibration of water, H_2O (0,0,1), prepared by infrared excitation. The theoretical results have also been compared to the results of Crim and co-workers on vibrationally mediated photodissociation of H_2O in which a higher overtone containing four quanta of O–H stretching is excited.[15] It has been shown that the rotational distribution described by the FC theory reproduces the experimental distribution obtained in the state-to-state experiments in which single rotational states were prepared.[9,15]

In the recent review of Engel *et al.*[2] it is stated that, "If there would not be the most recent experiments [of Mikulecki *et al.*[11]] we could without risk claim that the *ab initio* calculations··· reproduce essentially all experimental data on a quantitative level." Indeed, the recent measurements concerning the degree of vibrational excitation[11,12] which disagree with earlier measurements[3,8] and calculations[4] point to the fact that additional independent experiments are needed in order to investigate the agreement with the theoretical results.

In the present study we excite the symmetric stretch vibration of water, H_2O (1,0,0), and extend the approach of Hausler *et al.*[9] who excited the antisymmetric stretch. Recently we have utilized stimulated Raman excitation (SRE) to prepare densities of excited molecules in particular rovibrational states that are sufficient for studies of mode selective chemistry and molecular dynamics.[16] SRE combined with coherent anti-Stokes Raman scattering (CARS) allows preparation and detection, respectively, of single rotational states of H_2O, (1,0,0).[17] In the present experiments these methods, combined with LIF detection of OH, are used for monitoring the product state distributions of the OH species which are exclusively formed from 193 nm photodissociation of particularly selected rotational states of the H_2O with about $\sim 3657\ cm^{-1}$ of vibrational energy. Also, the rotational distribution resulting from photodissociation at 193 nm of ground vibrational state molecules is obtained. Our results show that at this photodissociation wavelength the dissociation cross section increases for vibrationally excited molecules compared to that from ground vibrational state molecules. Furthermore, the rotational-state distribution of the OH fragments depends on the initial rotational state of water. These measurements are an additional check point for comparison with the theoretical predictions.[2–4,9]

II. EXPERIMENT

The experimental protocol is described in Fig. 1. It involves excitation of a specific rovibrational state in the fundamental symmetric stretch vibration of H_2O, photolysis of the vibrationally excited molecule, and LIF detection[18] of OH. Vibrational excitation of H_2O (1,0,0) is effected by SRE, and the excited molecules are monitored by CARS.

The experimental setup is depicted in Fig. 2. The SRE is effected by tuning the frequency difference of two visible lasers to rotational transitions of the ν_1 band of H_2O

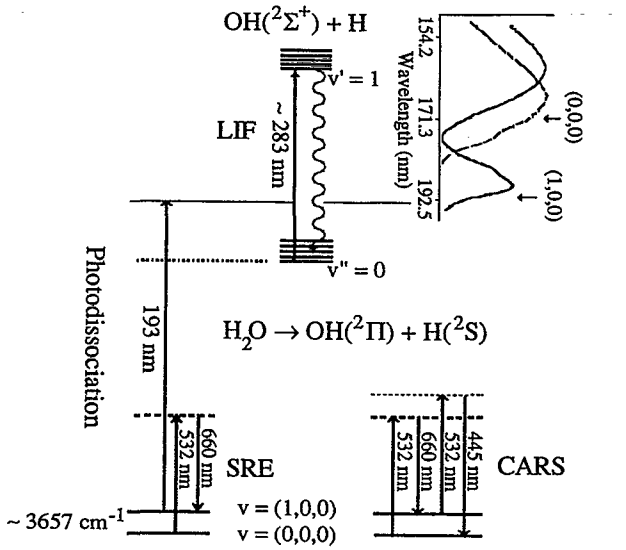

FIG. 1. Scheme of the experiment for the photodissociation of H_2O (1,0,0). $\sim 3657\ cm^{-1}$ corresponds to the excitation of ground vibrational state molecules to H_2O (1,0,0) via SRE. The vibrationally excited state of the water molecule is subsequently photodissociated using 193 nm photons and the OH products are detected by LIF. At the upper right corner the calculated absorption curves of H_2O (0,0,0) and H_2O (1,0,0) are shown. These curves are adapted from Ref. 4.

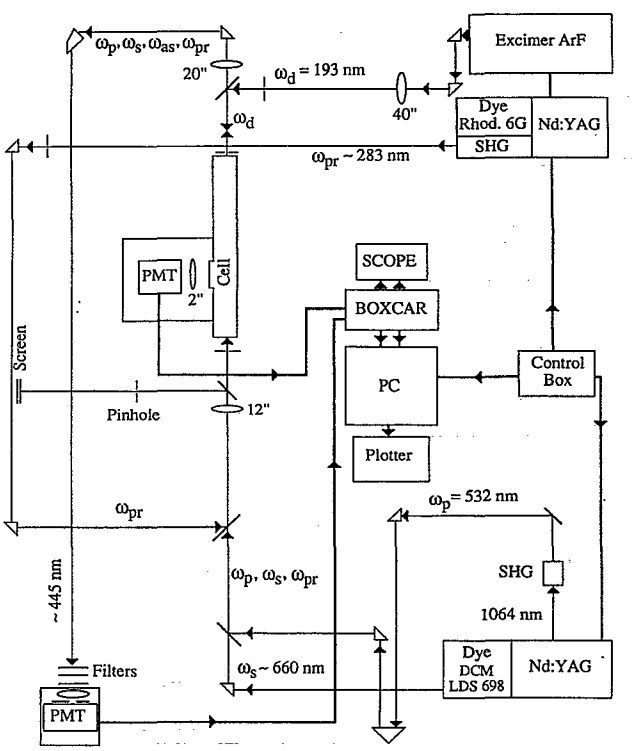

FIG. 2. Schematic drawing of the experimental setup, ω_p, ω_s, ω_{as}, ω_d, and ω_{pr} are the pump, Stokes, anti-Stokes, photodissociation, and probe wavelengths, respectively.

around 3650 cm^{-1}. The second harmonic of a Nd:YAG laser at 532 nm (ω_p) and a tunable dye laser (ω_s) pumped by it (Quantel, YG580, TDL50) provide the two visible beams necessary for the experiment. A mixture of DCM and LDS 698 allows generation of ~660 nm for H_2O (1,0,0) preparation. Typical ω_p energy is ~50 mJ and ω_s is ~6 mJ. Excitation of the molecule is monitored and optimized by measuring the CARS signal (ω_{as}) generated by the Raman excitation beams. Following the SRE pulse, after a delay of 30 ns, the rovibrationally excited molecules are photodissociated by a ~2 mJ, 193 nm beam (ω_d) from an ArF excimer laser (Lambda Physik, EMG 101MSC). After a delay of another 30 ns the OH photofragments are probed by LIF on the A, $v'=1\leftarrow X$, $v''=0$ transition,[19] with ~2–3 μJ, ~283 nm pulse (ω_{pr}) from the frequency-doubled output of a Nd:YAG-pumped dye laser (Quanta-Ray, DCR-2A, Lambda Physik, FL3002). The delays between the lasers are controlled by a digital delay generator (Stanford Research Systems, DG 535).

The ω_p, ω_s, and ω_{pr} beams propagate collinearly through the cell, after passing through a 12 in. focal length (f.l.) lens, which brings them to a common focus at the center of the cell axis. An optical delay line provides the temporal control necessary to keep the ω_p and ω_s pulses temporally overlapped. In order to check the spatial overlap of the three beams a small portion (~4%) of the beams is split off by a window and imaged onto a viewing screen, after passing through a pinhole located at the focus. At the exit of the gas cell ω_p, ω_s, ω_{pr}, and ω_{as} are transmitted by a dichroic mirror that reflects ω_d. The beams are recollimated by a 20 in. f.l. lens, then ω_{as} is separated from the input beams by a Pellin–Broca prism and color filters. A lens focuses ω_{as} onto a slit in front of a photomultiplier tube (PMT). The photodissociation beam ω_d counterpropagates, relative to the SRE and LIF beams, through a 40 in. f.l. lens which brings it to the focus of the other beams.

The LIF from the hydroxyl fragments is observed at a right angle to the laser beams and is imaged by a 2 in. f.l. f/1 lens onto a 5 mm slit in front of a PMT and an interference filter (310±5 nm). A boxcar integrator (Stanford Research Systems, SR250 and SR280) captures the resulting LIF and CARS signals. A PC controls the scanning of the dye laser. The LIF and CARS signals along with signals from photodiodes that monitor the energy of the photodissociation and probe lasers are analog to digital converted by a data acquisition and control board (Metrabyte, Dash-16) and accumulated pulse by pulse by the PC using the ASYST software.[20] Each data point in the ensuing spectra is obtained from these signals as an average of ten pulses. Also, all the data processing is carried out by using the ASYST software.

The probe pulse is kept at the above-mentioned low energy in order minimize saturation and to operate in the linear regime. The linear dependence of the LIF signal intensity on the probe pulse energy is tested for several transitions by inserting neutral density filters. However, some partial saturation is found by comparing the relative populations derived from different transitions that probe the same levels (the transitions assignment is taken from Ref. 19). Therefore, the fluorescence intensities are converted into relative populations by using a method that compensates for any degree of saturation.[21,22] This method incorporates a rate-equation analysis based on a simple "three level" system that considers the Einstein coefficients, radiative and nonradiative lifetimes, duration of the laser pulse, photodetection gate width, and the power density in the laser field. An effective power density is assumed and then changed until the populations derived from the different lines that probe the same levels agree (taking into account the available sets of main branches and satellites[19]). The effective power density that we find leads to consistent relative populations (within experimental errors). The Einstein coefficients used in this method are taken from Refs. 23 and 24.

The LIF signal and the effective probe power are normalized, point by point, to the photolysis and probe lasers energies, respectively. Since the CARS signal is saturated with respect to each of the exciting beams, the LIF signal is not normalized to it.

The experiments are carried out at room temperature in a gas cell through which the water vapor flows at a pressure of 0.1 Torr. The pressure and delays used in the experiments minimize collisional relaxation of the initially prepared H_2O states and the rotational states of the OH fragments. It has been found[25,26] that the most important self relaxation of H_2O (1,0,0) is to H_2O (0,0,1) with a rate constant of $\sim 3.1\times10^{-10}$ $cm^3\,s^{-1}$. This means that only 3% of the prepared H_2O molecules are relaxed vibrationally in our experiments. Using the measured rotational relaxation rate constant[27] for OH (X, $v''=0$) by H_2O, $2.2\pm0.5\times10^{-10}$ $cm^3\,s^{-1}$, we calculate that only 2% of the OH fragments are relaxed rotationally in our experiments. By carrying out the experiments under these conditions it is possible to measure the initial rotational state populations of the OH products.

Three types of experiments are conducted with this system. In the first, the probe laser wavelength is varied and the SRE laser kept fixed on a particular rovibrational transition of H_2O. This procedure yields OH LIF product excitation spectra from which the distribution of products among their quantum states can be extracted. In this case the CARS signal is used to identify and to optimize the SRE excitation of a particular Raman transition. Most of the state-to-state results reported below are obtained using this method. In the second type of experiment we monitor particular OH rotational states at fixed LIF wavelength while varying the SRE laser wavelength to generate a reactant state yield spectrum, that is a spectrum of the H_2O molecules that photodissociate to produce OH fragments in the specific quantum state. In the third type of experiment the SRE beams are turned off for the photodissociation of H_2O (0,0,0). Because of the weak signal in the last type of experiment the pressure is increased to 0.2 Torr keeping similar delays between the photolysis and probe lasers (even at this pressure less then 5% of the OH products are relaxed rotationally).

III. RESULTS

We start this section by briefly summarizing the spectroscopy of the H_2O and OH species.

The Raman transitions used for the SRE are[28]

$$H_2O(0,0,0)J_{K_aK_c} \rightarrow H_2O(v_1,v_2,v_3)J'_{K'_aK'_c}, \quad (1)$$

where (v_1,v_2,v_3) are the quantum numbers for vibration and J, K_a, and K_c are the quantum numbers for the total angular momentum and its projection on the a and c axes in the prolate and oblate symmetric limits. The water molecule is an asymmetric top and has a complicated structure of its rovibrational levels. Each rotational level consists of $2J+1$ sublevels; in addition, each sublevel possesses the usual $2J+1$ magnetic degeneracy (m quantum number). Sublevels with different J overlap and the resulting CARS spectrum is complicated and not completely rotationally resolved. The assignment of the rotational transitions used to prepare the initial states for the dissociation is carried out by comparison of the experimental and calculated spectra as reported in our recent CARS studies on the streching vibrations of the water isotopomers.[17] All the transitions belong to the isotropic Q branch, i.e., they are between rotational levels that have the same quantum numbers. Resolved transitions that select particular rotations can be used to prepare the initial states in the experiments. Unfortunately, with the overall CARS spectral resolution that we calculated from our laser specifications, 0.16 cm^{-1}, many of the transitions overlap. Therefore, four different transitions are chosen: two of the transitions prepare single rotational states, the 1_{01} and 3_{03} states; the other two combine two states, $1_{10}+1_{11}$ and $2_{12}+2_{11}$, where in each case the first transition is dominant due to the different nuclear spin statistical weight (a ratio 3 to 1).[17] These rotational states are very close in energy but they represent different J's. Other transitions are not used since they involve more than two states or they are too weak.

The photodissociation of H_2O (0,0,0) and the photodissociation of particularly selected rotational states of the H_2O (1,0,0) produces the OH ($X\,^2\Pi$) fragment which has an unpaired $p\pi$ electron in the outer shell with electronic angular momentum $\Lambda=1$ and spin $S=1/2$. The spin–orbit coupling gives rise to two multiplet states, $^2\Pi_{3/2}$ and $^2\Pi_{1/2}$, which are split by about 126 cm^{-1} for the first rotational levels.[19,29] The rotational energy levels are designated by N, the total angular momentum quantum number without spin. The OH total angular momentum, J, is equal to $N+1/2$ and $N-1/2$ for the $^2\Pi_{3/2}$ and $^2\Pi_{1/2}$ states, respectively. Due to the coupling between the rotation of the OH and the electronic orbital motion each rotational level is split to two Λ-doublet components which are only about 0.03–3 cm^{-1} apart for $N=1$ to 8.[19,29] The Λ-doublet electronic wave functions are symmetric and antisymmetric with respect to reflection in the plane of rotation of the OH and are designated by A' and A'', respectively.[30]

In order to obtain the rotational distribution and the spin and Λ-level populations we use the P, Q, and R main and satellite transitions observed in the LIF spectrum. Q lines monitor the A'' state, while the P and R lines monitor the A' state. Each point in Figs. 3–6 and 9–12 which are presented below is the result of an average of five spectra.

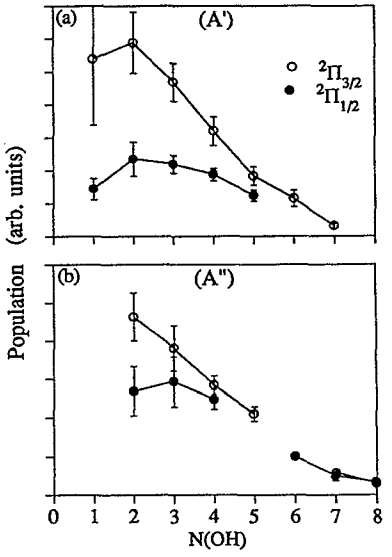

FIG. 3. Population of product rotational states for the photodissociation of ground vibrational state water molecules shown for the $^2\Pi_{3/2}$ (open circles) and $^2\Pi_{1/2}$ (closed circles) states in the Λ-doublet A' state (a) and A'' state (b).

A. Photodissociation of H_2O (0,0,0)

A small LIF signal of the OH is obtained even when the SRE beams are off. This signal results from the photodissociation of ground vibrational state molecules. Although the absorption cross section of H_2O (0,0,0) at 193 nm ($\sim 1.5\times10^{-21}$ cm^2) is very small[31] the LIF signal of the OH product is sufficient to determine its rotational distribution.

Shown in Fig. 3 are the OH product rotational distributions obtained in the photodissociation of all occupied rotational states of H_2O (0,0,0) at room temperature. The distributions are given for the two Λ-doublet components and for both spin–orbit states. The distributions are smooth with low rotational excitation and a peak at $N=2$. In the A'' distributions few data points are missing due to overlap of too many lines in the LIF spectrum. For $^2\Pi_{1/2}(A')$, rotations with $N>5$ could not be reliably measured since the signal was too weak. The behavior of the two spin–orbit states seems similar within the experimental errors when the different statistical weights of the two states are accounted for. The ratios of the population of the two spin–orbit states are given in Fig. 4 for both Λ-doublet components. Small preference of the $^2\Pi_{3/2}$ state can be seen for the A' component, but the errors are very large here. For the A'' component the distribution between the spin–orbit states is certainly statistical.

The OH population in both Λ-doublet components is of a Boltzmann type as shown in Fig. 5 for both spin–orbit states. Rotational "temperatures" of 361 ± 13 and 465 ± 10

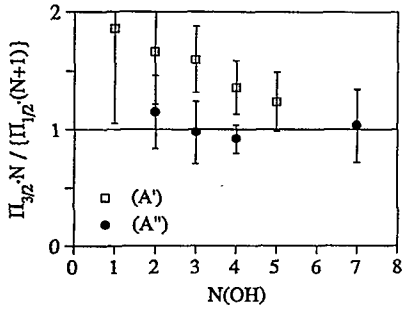

FIG. 4. Spin state distribution in the OH product resulting from photodissociation of H_2O (0,0,0) for the Λ-doublet states: A' (open squares) and A'' (closed circles).

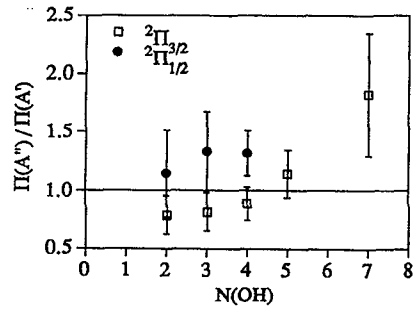

FIG. 6. The Λ-doublet ratio for the photodissociation of H_2O (0,0,0) at 193 nm for the $^2\Pi_{3/2}$ state (open squares) and for the $^2\Pi_{1/2}$ state (closed circles).

K for the $^2\Pi_{3/2}$ state and of 392 ± 13 and 468 ± 19 K for the $^2\Pi_{1/2}$ state are obtained for the A' and A'' Λ-doublet components, respectively.

Figure 6 shows the ratios of the populations of the two Λ-doublet components for the $^2\Pi_{3/2}$ and $^2\Pi_{1/2}$ spin–orbit states. Although the distribution is close to statistical, it can be seen that the ratio $\Pi(A'')/\Pi(A')$ tends to increase with increasing N for the $^2\Pi_{3/2}$ state.

B. State-to-state photodissociation of H_2O (1,0,0)

The CARS spectrum that monitors the excitation of the H_2O (1,0,0) is shown in panel (a) of Fig. 7. Panel (b) presents the OH LIF signal, following the photodissociation of the H_2O, as a function of the SRE scan with the probe laser fixed on the $P_1(2)$ OH transition. The labels in panel (a) mark the rotational transitions used to prepare the initial states for the state-to-state experiments described below. It is clearly seen that the LIF signal tracks the CARS signal. Thus the production of the OH fragments is enhanced by the H_2O (1,0,0) excitation. The enhancement is very large, leading to ~8–10 times stronger LIF signal from the photodissociation of particular rotational states of H_2O (1,0,0) than that from ground vibrational state molecules. The background signal due to photodissociation of

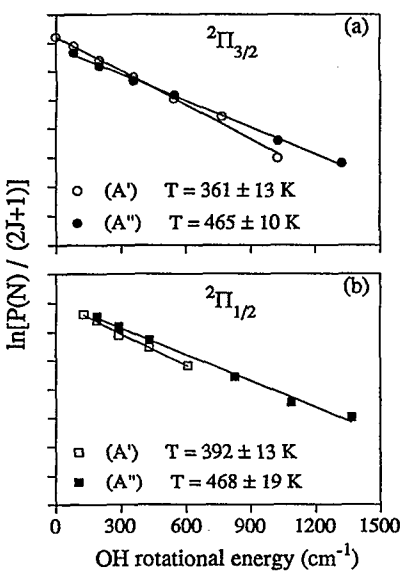

FIG. 5. Boltzmann plot of the rotational-state distribution of the OH photofragments from photodissociation of H_2O (0,0,0) for (a) the $^2\Pi_{3/2}(A')$ (open circles) and (A'') state (closed circles) and for (b) the $^2\Pi_{1/2}(A')$ (open squares) and (A'') state (closed squares). The temperature is calculated from the slope.

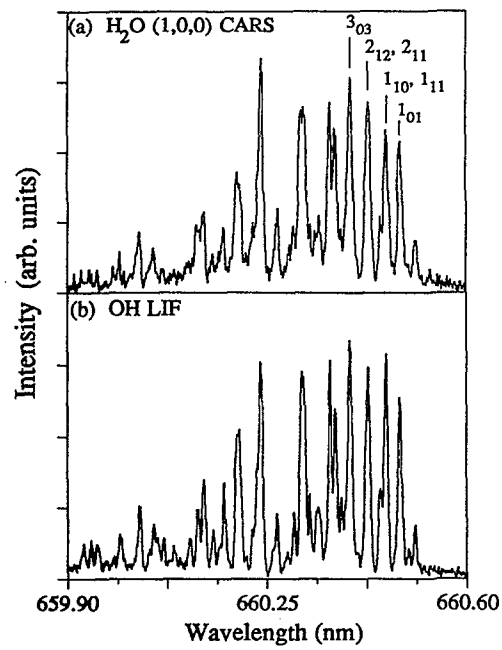

FIG. 7. (a) The saturated CARS signal from H_2O (1,0,0) obtained by scanning the SRE laser over the rotational levels. The peaks correspond to the isotropic Q-branch rotational transitions (Ref. 17), and the marked peaks to the rotational transitions used to prepare the initial states for the study of the OH distribution. (b) LIF of the $P_1(2)$ transition of the OH fragments as a function of the rotational excitation of the photodissociated H_2O (1,0,0).

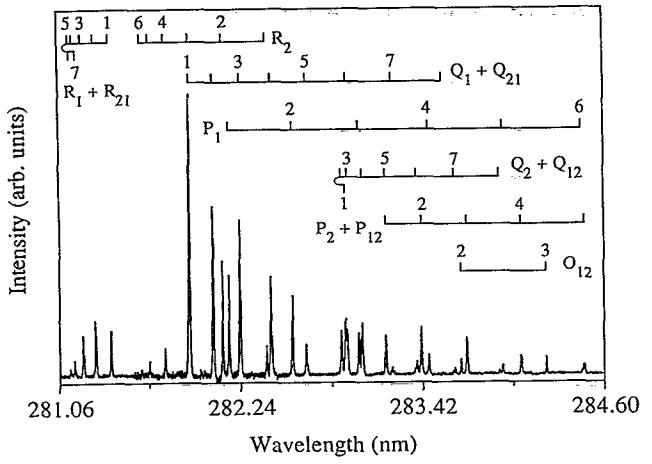

FIG. 8. LIF excitation spectrum of the OH photoproducts (measured for the transition A, $v'=1\leftarrow X$, $v''=0$) resulting from the photodissociation of the 3_{03} rotational state of H_2O (1,0,0). The assignment of the transitions is based on Ref. 19.

H_2O (0,0,0), which is negligible comparable to the signal resulting from H_2O (1,0,0), has not been subtracted.

The LIF excitation spectrum of the OH photofragments, measured for the A, $v'=1\leftarrow X$, $v''=0$ transition between 281.06–284.60 nm in the first type of experiment, is shown in Fig. 8 for photodissociation from the 3_{03} rotational state of H_2O (1,0,0). Similarly, LIF excitation spectra of OH are obtained for the photodissociation resulting from the other three initial rotational states 1_{01}, $1_{10}+1_{11}$ and $2_{12}+2_{11}$ of the H_2O (1,0,0). By using the available data from these spectra, the OH rotational distributions are extracted for the photodissociation from each of the initial rotational states. As mentioned above, in each of the two combined transitions the first component (1_{10} and 2_{12}, respectively) is dominant.

The OH rotational distributions for the two Λ-doublet components for each of the two spin–orbit states are shown in Fig. 9 for the photodissociation of the particular initial rotational states of H_2O (1,0,0). Fig. 9(A) shows the distributions resulting from dissociation of the 1_{01} and 3_{03} and Fig. 9(B) of the $1_{10}+1_{11}$ and $2_{12}+2_{11}$ initial states. The

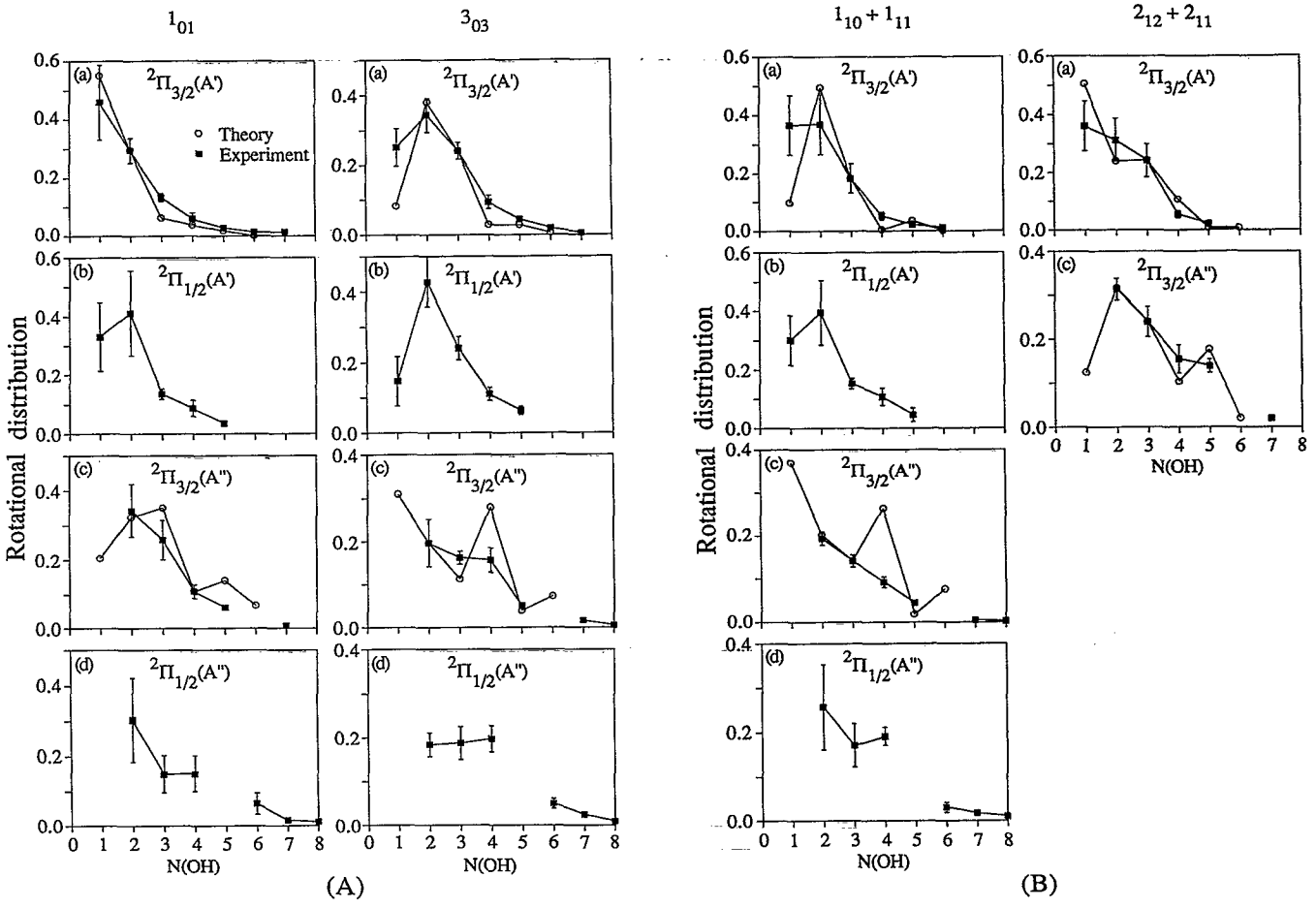

FIG. 9. Measured (closed squares) and calculated (open circles) product rotational-state distributions for the photodissociation of H_2O (1,0,0) molecules of (A) the 1_{01} and 3_{03} and of (B) the $1_{10}+1_{11}$ and $2_{12}+2_{11}$ rotational states: (a) $^2\Pi_{3/2}(A')$, (b) $^2\Pi_{1/2}(A')$, (c) $^2\Pi_{3/2}(A'')$, and (d) $^2\Pi_{1/2}(A'')$. The experimental distributions in the four panels are normalized to unity. The scale of the theoretical results is normalized to the experiments separately for each Λ-doublet component. The calculations from Ref. 9 are for photodissociation of H_2O (0,0,1) and are given only for the $^2\Pi_{3/2}$ state.

distributions of the two Λ-doublet components of the $^2\Pi_{3/2}$ state are shown along with the calculations of Ref. 9 which are based on the FC theory. In Fig. 9(B) the relative contributions of the components of the initial states have been accounted for in the theoretical distributions. As in the case of the photodissociation of H_2O (0,0,0), here too only low OH rotational levels are populated. However, the distributions are structured and depend on the particular rotational state that is photodissociated, in contrast to the smooth distributions resulting from the photodissociation of H_2O (0,0,0). Reasonably good agreement is found between the theory and the OH rotational distributions obtained from the H_2O (1,0,0) photodissociation.

Although a nonstatistical distribution is observed for both Λ-doublet components, the population of the OH fragments can be fitted on a Boltzmann plot when averaged over the two components. Furthermore, most of the distributions can still be approximately fitted on a Boltzmann plot even for each Λ-doublet component separately. The latter fitting always yields higher "temperature" for the A'' Λ-doublet component. The rotational temperatures obtained for the average of the A'' and A' Λ-doublet components of the $^2\Pi_{3/2}$ spin state are given in Fig. 10. Panels (a)–(d) show the results of the state-to-state photodissociation of H_2O (1,0,0) and panel (e) the results for H_2O (0,0,0) for comparison. The state-to-state plots are presented in an increasing order of their initial rotational-state energy. The rotational temperatures depend on the initial H_2O (1,0,0) rotational states and in general increase with their rotational energy.

The population ratios of the two spin–orbit states for the state-to-state dissociations are shown in Fig. 11 for the two Λ-doublet components. Within our experimental errors and with very few points of exception, all the spin distributions are close to statistical.

Shown in Fig. 12 are the Λ-doublet ratios for the $^2\Pi_{3/2}$ and $^2\Pi_{1/2}$ spin–orbit states along with the theoretical prediction for the $^2\Pi_{3/2}$ state,[9] for the photodissociation of the four different initial H_2O (1,0,0) states. While only a small preference of the A'' component at high OH rotational quantum numbers is found for photodissociation of H_2O (0,0,0), all state-to-state experiments in H_2O (1,0,0) show very clear N-dependent preferential population for the A'' component where the ratio $\Pi(A'')/\Pi(A')$ approaches values of ~6. Note that in panels (c) and (d) no theoretical data is given for the OH rotational quantum numbers $N=4$ and $N=5$, respectively. This is because theory predicts almost no population in the A' component of these rotational quantum states and as a result very large ratios of the Λ-doublet components (with large errors) are obtained. It is clearly seen that for all the photodissociated initial states, the state-to-state calculations predict higher values and much more pronounced "structure" of the Λ-doublet ratios than is observed in our experiments.

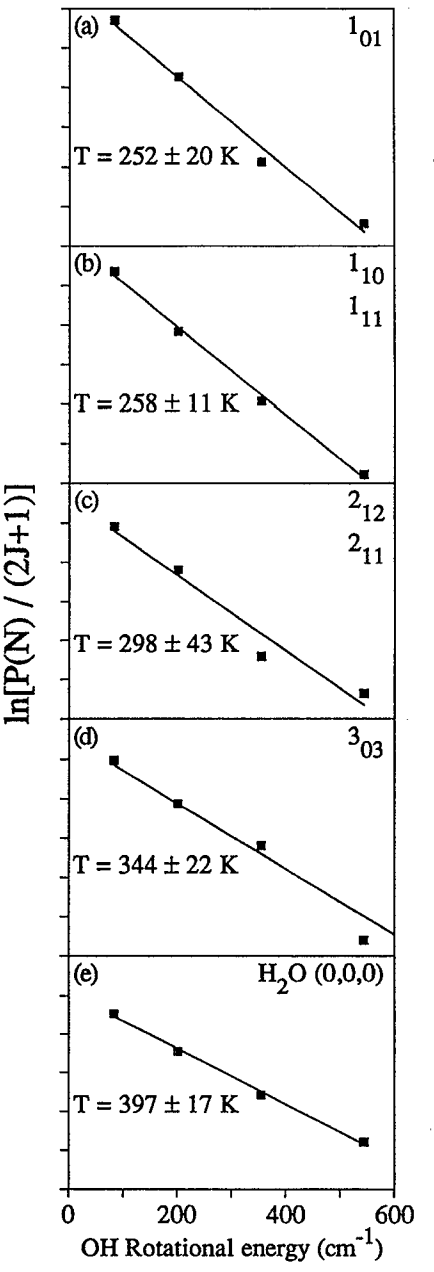

FIG. 10. Boltzmann plot of the population of the averaged Λ-doublet components of OH in the $^2\Pi_{3/2}$ state obtained from photodissociation of the initial rotational states of H_2O (1,0,0): (a) 1_{01}, (b) $1_{10}+1_{11}$, (c) $2_{12}+2_{11}$, (d) 3_{03}, and of H_2O (0,0,0) (e). The rotational temperatures are obtained from the slope of the corresponding lines.

IV. DISCUSSION

Our results clearly show that the production of the OH fragments is enhanced by the H_2O (1,0,0) excitation. The LIF signal resulting from the photodissociation of the particular rotational states of H_2O (1,0,0) increases ~8–10 times in comparison to that from H_2O (0,0,0). An estimate of the value of the cross section for photodissociation of the vibrationally excited molecules is obtained from the population in a particular H_2O (0,0,0) rotational state, the efficiency of vibrational excitation and the enhancement of the LIF signal. For example, at room temperature ~6% of the H_2O (0,0,0) molecules are in the 3_{03} rotational state and the enhancement in the LIF signal is ~10. From the measurements of Valentini and Tabor[32] we estimate 30%

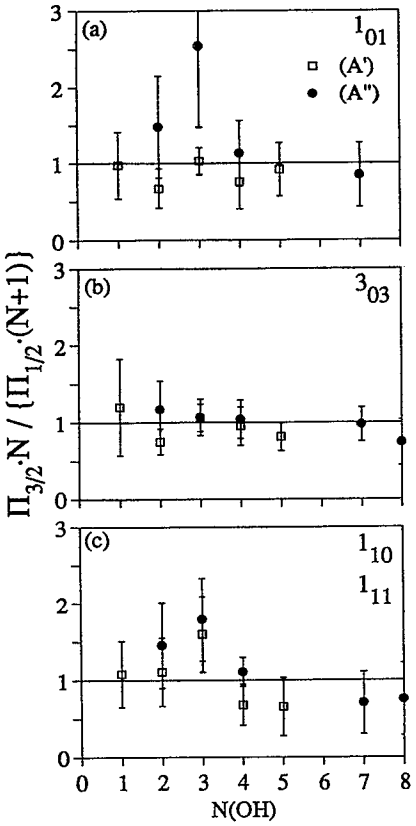

FIG. 11. Spin–orbit state distribution in the OH product resulting from photodissociation of H_2O (1,0,0): (a) 1_{01}, (b) 3_{03}, and (c) $1_{10}+1_{11}$ for the Λ-doublet states A' (open squares) and A'' (closed circles).

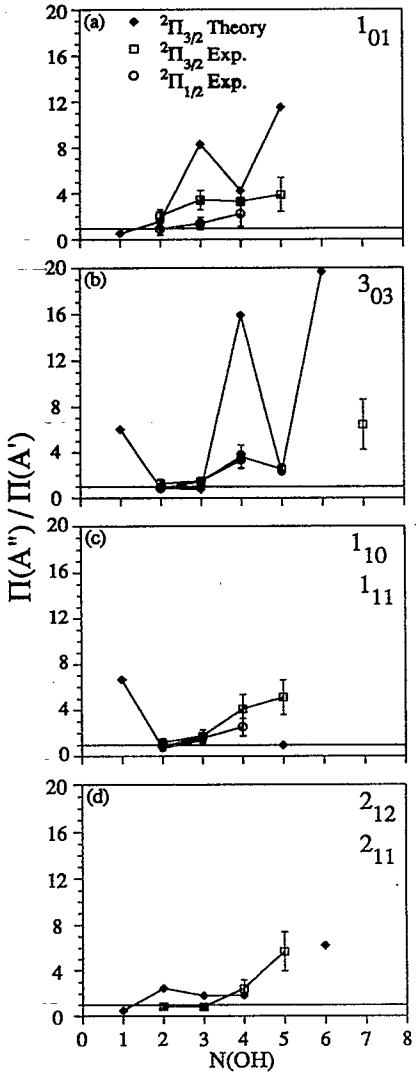

FIG. 12. The Λ-doublet ratio for the photodissociation of H_2O (1,0,0): (a) 1_{01}, (b) 3_{03}, (c) $1_{10}+1_{11}$, and (d) $2_{12}+2_{11}$ rotational states. Measured ratios are given for the $^2\Pi_{3/2}$ (open squares) and for the $^2\Pi_{1/2}$ (open circles) states along with calculated ratios for the $^2\Pi_{3/2}$ (closed rhombuses) state. The calculated values are obtained by taking the ratios of the populations given in Ref. 9 for the two Λ-doublet components.

SRE efficiency which implies that the cross section for photodissociation of H_2O (1,0,0) at 193 nm is ~550 times greater than that for ground vibrational state H_2O. Since the measured cross section for absorption of H_2O (0,0,0) at 193 nm is $\sim 1.5\times10^{-21}$ cm^2 (Ref. 31), we obtain a value of $\sim 0.8\times10^{-18}$ cm^2 for the absorption from H_2O (1,0,0). According to the theoretical calculations, the absorption cross section is a sensitive function of the particular excited vibrational state that is photodissociated and of the wavelength of photodissociation.[4] The H_2O (1,0,0) absorption cross section (see the right upper corner of Fig. 1) has a pronounced minimum around 175 nm and is different from that for H_2O (0,0,1) and (0,1,0).[4] Unfortunately, the calculations do not extend to the wavelength of 193 nm for the ground state molecules, and therefore it is impossible to obtain the theoretical ratio between the cross sections for absorption for H_2O (1,0,0) and H_2O (0,0,0). Also, enhancement of the absorption cross section, by the same order of magnitude, is found for the photodissociation of H_2O (0,0,1)[9] and HOD (0,0,1)[16] at 193 nm. We note that the studies where the fundamental stretching modes of the molecules are photodissociated are conducted at 193 nm. This is because at this wavelength the absorption cross section for photodissociation is much larger for vibrationally excited species than for ground vibrational state molecules and allows significant production of the photoproducts from particular rotational states.

The theoretical calculations reveal that FC effects are the source of the difference in photodissociation behavior of H_2O (0,0,0), H_2O (1,0,0), and H_2O (0,0,1). The enhancement of the photodissociation cross section of H_2O (0,0,1) and H_2O (1,0,0) is the result of a much better FC overlap of the dissociative continuum $A(^1B_1)$ with the (1,0,0) or (0,0,1) vibrational wave functions than with the (0,0,0) wave function. In the cases of H_2O (0,0,1) and H_2O (1,0,0), the better FC overlap enables the additional energy to enhance the photodissociation by extending the absorption spectrum to longer wavelengths. The FC effects

are also the source of the bond selectivity in the fragmentation of HOD (0,0,1), where the FC overlap of the (0,0,1) wave function with the OH+D continuum is better than with the OD+H continuum,[16] leading to enhancement of the products resulting from the former dissociation channel.

The present experimental results of the photodissociation of H_2O (0,0,0) are similar to the results of some previous works.[9,10] The OH resulting from H_2O (0,0,0) photodissociated molecules shows a smeared rotational distribution peaking at $N=2$. This behavior is also consistent with the predictions of Guo and Murrell,[33] based on classical dynamics calculations of H_2O (0,0,0) photodissociation at 193 nm.

As shown above (Fig. 5), the rotational temperatures resulting from photodissociation of H_2O (0,0,0) are 361 $\pm$13 and 465$\pm$10 K for the $^2\Pi_{3/2}$ state and 392$\pm$13 and 468$\pm$19 K for the $^2\Pi_{1/2}$ state for the A' and A'' Λ-doublet components, respectively. These temperatures show a general trend in which the A' component is colder than the A'' component for the two spin–orbit states. The higher rotational temperature of the A'' state points to the fact that this Λ-doublet component is slightly preferred in comparison to the A' state. This behavior has already been observed by Hausler *et al.*[9] for the $^2\Pi_{3/2}$ component resulting from the 193 nm photodissociation of H_2O (0,0,0) and by Andresen *et al.*[10] in the 157 nm photodissociation of cold water.

The state-to-state photodissociation of H_2O (1,0,0) shows a structured OH rotational distribution for the two Λ-doublet components, which depends on the particular rotational state of H_2O (1,0,0). This behavior is different from that observed in the photodissociation of ground vibrational state molecules where smooth OH distributions are obtained due to the averaging resulting from the photodissociation of all the occupied rotational states at room temperature.

A reasonably good agreement is found between the FC theoretical calculations[2,9] and the OH rotational distribution obtained from the H_2O (1,0,0) photodissociation. The final rotational distributions can be described within the FC limit in the absence of translational–rotational coupling in the exit channel.[2] The FC theory predictions are for photolysis of selected rotational states of H_2O (0,0,1). In these calculations the OH rotational distribution is independent of the H_2O stretching motion due to the assumption of separability of the radial and angular wave functions of the ground and electronically excited states. Good agreement with theory has previously been obtained for the photolysis of water from initial rotational states prepared via excitation of the fundamental asymmetric stretch vibration,[9] and via excitation of an overtone containing four quanta of O–H stretching.[15] However, it is important to note that generally the structured rotational distribution is much more pronounced in the theory than in the present as well as in the previous[9,15] state-to-state experimental studies. These experimental results demonstrate that the final OH rotational distributions are controlled by the initial rotational motion of the water molecule and that the amount of the initial stretching excitation has negligible influence and therefore justify the separability assumption in the FC calculations. It should be mentioned here that the H_2O bending excitation has strong influence on the OH product rotational distributions.[34,35]

Although a nonstatistical distribution is observed for both Λ-doublet components, the population of the OH fragments when averaged on the A'' and A' Λ-doublet components can be fitted on a Boltzmann plot. As shown in panels (a)–(d) of Fig. 10, rotational temperatures in the range of 250 to 350 K are obtained using this averaging for the state-to-state experiments. These rotational temperatures depend on the initial H_2O (1,0,0) rotational states and in general increase with their rotational energy. This trend was also observed by Hausler *et al.*[9] in their experiments on the photodissociation of H_2O (0,0,1). Our values, which are all for $J=1$ to $J=3$ initial rotational states, are higher than those for the 0_{00} state, but lower than for the $J=4$ states measured by Hausler *et al.*[9] The temperature obtained by the same averaging for the H_2O (0,0,0) dissociation, 397$\pm$17 K [Fig. 10, panel (e)], is close to that for the 3_{03} state which is the most populated rotational state of the water molecule at room temperature. From the dependence of the OH rotational temperature on the prepared initial rotational state it is obvious that at least part of the rotational energy contents in the photodissociated water molecule is transferred to the product OH. As mentioned above, most of the OH rotational distributions can still be approximately fitted on a Boltzmann plot even for each Λ-doublet component separately, despite their structured behavior. The fitting always yields higher temperature for the A'' Λ-doublet component. This trend was also found in the 193 nm photodissociation of H_2O (0,0,0)[9] and in the 157 nm photodissociation of cold water.[10] It is worth noting that the calculated rotational distributions could not be described even approximately on a Boltzman plot since their structure is much more pronounced.[9]

The population ratios of the two spin–orbit states of OH for the ground vibrational state and the state-to-state photodissociation are shown in Figs. 4 and 11, respectively. Within our experimental errors and with very few points of exception, the spin distributions are close to statistical. This behavior is expected from the FC theory[2] and is consistent with the results of all other experiments of H_2O photodissociation.[2,3,8–11] Thus the photodissociation process does not distinguish between the two spin–orbit states.

The ratio of the populations of the two Λ-doublet components is shown in Figs. 6 and 12 for the two spin–orbit states for the photodissociation of H_2O (0,0,0) and H_2O (1,0,0), respectively. The theoretical prediction for the ratio in the $^2\Pi_{3/2}$ state for the photodissociation of H_2O (0,0,1)[9] is shown in Fig. 12. The Λ-doublet ratio shows preference of the A'' component for photodissociation from selected rotational states, while only a small preference at high N is observed for photodissociation from the ground vibrational state.

Strong N-dependent preference of the A'' component has previously been found in the dissociation of cold H_2O at 157 and 193 nm,[8–10] while no or only small preference

was found in the room temperature dissociation at 157 and 193 nm.[2,8–10] The preference of the A'' component is explained qualitatively by the conservation of the electronic symmetry in the break up of the excited transition complex. The $A\,^1B_1$ state of the dissociating molecule is antisymmetric, while the formed hydrogen atom ($^2S_{1/2}$ state) is symmetric and therefore the OH must be formed in the antisymmetric A'' state. However, assignment of the two Λ-doublet states as the antisymmetric A'' and the symmetric A' states is a good approximation only for high N's.[2,8] For low and intermediate N's, Λ-doublet mixing occurs between the two components, leading to the N dependence preference.

Also, when photodissociating all rotational states of a room temperature sample, the initial out-of-plane rotations of the H_2O (0,0,0) disturb the Λ-doublet preference,[8] and therefore the photodissociation in this case leads only to a small preference, even for high N's. On the other hand, it is expected that for the photodissociation of H_2O from the 1_{01} and 3_{03} states, which are pure in-plane rotations,[36] the A'' state will be preferentially populated. Although in the photodissociation from $1_{10}+1_{11}$ states there is a dominant contribution of an out-of-plane rotation (1_{10}), it seems that for this value of J the period of rotation is too low to destroy the A'' preference. For the H_2O photodissociation from the $2_{12}+2_{11}$ states the motion is close to in-plane and leads to A'' preference. Since the state-selected photodissociation of H_2O leads to significant A'' preference while in the photodissociation of H_2O (0,0,0) at room temperature only small preference is observed even for high N's, it might be anticipated that photodissociation from some rotational states of H_2O leads to A' preference (see below).

The state-to-state calculations of Hausler *et al.*[9] predict a complicated behavior of the Λ-doublet states population and a preference which is dependent on the selected state of H_2O and the N rotational quantum number of OH. Applying the prediction to the states photodissociated in our experiment results in a much more pronounced structure and preference of the A'' state than is obtained in the experiment. It is worth noting that the calculations predict preference (for almost all N's) of the A' state in photodissociation of selected states of H_2O such as 3_{30} and 3_{31} which we could not measure due to weak signal and overlap problems.

V. CONCLUSIONS

The photodissociation of H_2O prepared in particular rotational states of the symmetric stretch vibration, photolyzed with 193 nm light and detected by LIF of the OH fragments, has been investigated. Our results show that specific energy deposition via the lowest level of vibrational excitation leads to the enhancement of bond breaking. This enhancement results from the increase of the photodissociation cross section from vibrationally excited molecules compared to that from ground vibrational state molecules. Due to difference in the reflection of the (1,0,0) and (0,0,0) states at the repulsive dissociative surface, different FC overlaps are obtained and the better FC overlap in the photodissociation of the (1,0,0) enhances the photodissociation.[16] The ratio between the photodissociation cross section of vibrationally excited molecules and of ground vibrational state molecules can not be compared to theoretical calculations since they are not available for the latter at this photodissociation wavelength.

The state-to-state photodissociation of H_2O demonstrates the importance of initially selected wave functions in controlling the dissociation. The preparation of the fundamental symmetric stretch by SRE extends the studies in which the fundamental asymmetric stretch and the state containing four OH stretching quanta were prepared by infrared[9] and visible excitation,[15] respectively. All these methods facilitate state-to-state photodissociation studies and comparison with theoretical predictions. Relying on the experimental results, it is concluded that excitation of particular rotational states in different nuclear motions leads to rotational state distributions of OH that are structured and dependent on the prepared rotational state of the vibrationally excited H_2O, but independent of the stretching mode. These findings strenghten the assumption of the separability of the radial and angular wavefunctions of the ground and electronically excited states in the FC theory.

Although the structured rotational distribution is less pronounced in the experimental results than in the theoretical predictions of the FC model, the agreement between experiment and theory is reasonably good. Furthermore, comparison of the population ratio of the two Λ-doublet components to the theoretical results also demonstrates only qualitative agreement. The fact that the agreement is only qualitative is reasonable since the theoretical model takes into account only the projection of the ground on the excited electronic state and does not include any estimate of the translational–rotational coupling in the exit channel. Therefore, it is possible that the deviation of the measured distributions from the FC theoretical results manifests the influence of the exit channel coupling. We may speculate that in order to get a better agreement with the theoretical results the theoretical model has to be refined.

The Λ-doublet ratio shows only a small preference at high N of the A'' component in the photodissociation of ground state molecules at 193 nm, while a much stronger preference is observed in the state-selected photodissociation of H_2O (1,0,0). This preference is dependent on the particular rotational state that is photodissociated and on the N quantum number. Since the preference of the A'' component in photodissociation of H_2O (0,0,0) is small we conclude that photodissociation from other particular states may lead to A' preference. The FC calculations suggest that the 3_{30} and 3_{31} states show A' preference. In order to obtain the A' preference one should photodissociate the water molecules from the above-mentioned states.

ACKNOWLEDGMENTS

This work is supported by a grant from the Hasselblad Foundation. We thank J. A. Beswick and J. J. Valentini for helpful discussions.

[1] H. Okabe, *Photochemistry of Small Molecules* (Wiley, New York, 1978).

[2] V. Engel, V. Staemmler, R. L. Vander Wal, F. F. Crim, R. J. Sension, B. Hudson, P. Andresen, S Hennig, K. Weide, and R. Schinke, J. Phys. Chem. **96**, 3201 (1992), and references cited therein.
[3] P. Andresen and R. Schinke, in *Molecular Photodissociation Dynamics*, edited by M. N. R. Ashfold and J. E. Baggott (Royal Society of Chemistry, London, 1987), p. 61.
[4] V. Engel, R. Schinke, and V. Staemmler, J. Chem. Phys. **88**, 129 (1988); V. Engel and R. Schinke, *ibid.* **88**, 6831 (1988).
[5] K. S. Sorbie and J. N. Murrell, Mol. Phys. **29**, 1387 (1975); **31**, 905 (1976).
[6] V. Stammler and A. Palma, Chem. Phys. **93**, 63 (1985).
[7] H.-T. Wang, W. S. Felp, and S. P. McGlynn, J. Chem. Phys. **67**, 2614 (1977).
[8] P. Andresen, G. S. Ondrey, B. Titze, and E. W. Rothe, J. Chem. Phys. **80**, 2548 (1984); P. Andresen and E. W. Rothe, *ibid.* **82**, 3634 (1985).
[9] D. Hausler, P. Andresen, and R. Schinke, J. Chem. Phys. **87**, 3949 (1987).
[10] A. U. Grunewald, K. H. Gericke, and F. J. Comes, Chem. Phys. Lett. **133**, 501 (1987).
[11] K. Mikulecky, K. H. Gericke, and F. J. Comes, Chem. Phys. Lett. **182**, 290 (1991); Ber. Bunsenges. Phys. Chem. **95**, 927 (1991).
[12] D. David, I. Bar and S. Rosenwaks (unpublished).
[13] G. G. Balint-Kurti, J. Chem. Phys. **84**, 4443 (1986).
[14] R. Schinke, V. Engel, P. Andresen, D. Hausler, and G. G. Balint-Kurti, Phys. Rev. Lett. **55**, 1180 (1985).
[15] R. L. Vander Wal, J. L. Scott, and F. F. Crim, J. Chem. Phys. **94**, 1859 (1991).
[16] I. Bar, Y. Cohen, D. David, T. Arusi-Parpar, S. Rosenwaks, and J. J. Valentini, J. Chem. Phys. **95**, 3341 (1991); Y. Cohen, D. David, T. Arusi-Parpar, I. Bar, S. Rosenwaks, and J. J. Valentini, in *Mode Selective Chemistry*, edited by J. Jortner, R. D. Levine, and B. Pullman (Kluwer, Dordrecht, 1991), p. 227; I. Bar, Y. Cohen, D. David, S. Rosenwaks, and J. J. Valentini, J. Chem. Phys. **93**, 2146 (1990).
[17] D. David, A. Strugano, I. Bar, and S. Rosenwaks, Appl. Spectrosc. **46**, 1149 (1992).
[18] J. L. Kinsey, Ann. Rev. Phys. Chem. **28**, 349 (1977).
[19] G. H. Dieke and H. M. Crosswhite, J. Quantum. Spectrosc. Radiat. Transfer **2**, 97 (1962).
[20] ASYST Software Technologies Inc., Rochester, N.Y., Versions 2.10 and 3.10, 1989.
[21] J. F. Cordova, C. T. Rettner, and J. L. Kinsey, J. Chem. Phys. **75**, 2742 (1981).
[22] S. Zabarnick, J. W. Fleming, and A. P. Baronavski, J. Chem. Phys. **85**, 3395 (1986).
[23] W. L. Dimpfl and J. L. Kinsey, J. Quant. Spectrosc. Radiat. Transfer. **21**, 233 (1979).
[24] I. L. Chidsey and D. R. Crosley, J. Quant. Spectrosc. Radiat. Transfer. **23**, 187 (1980).
[25] J. Finzey, F. E. Hovis, V. N. Panfilov, P. Hess, and C. B. Moore, J. Chem. Phys. **67**, 4053 (1977).
[26] P. F. Zittel and D. E. Masturzo, J. Chem. Phys. **90**, 977 (1989).
[27] K. H. Gericke and F. J. Comes, Chem. Phys. **65**, 113 (1982).
[28] G. Herzberg, *Molecular Spectra and Molecular Structure II. Infrared and Raman Spectra* (Van Nostrand, New York, 1945).
[29] G. Herzberg, *The Spectra and Structure of Simple Free Radicals* (Cornell University, Ithaca, 1971).
[30] M. H. Alexander, P. Andresen, R. Bacis, R. Bersohn, P. J. Dagdigian, F. J. Comes, R. N. Dixon, R. W. Field, G. W. Flynn, K.-H. Gericke, E. R. Grant, B. J. Howard, J. R. Huber, D. S. King, J. L. Kinsey, K. Kleinermanns, K. Kuchitsu, A. C. Luntz, A. J. McCaffery, B. Pouilly, H. Reisler, S. Rosenwaks, E. W. Rothe, M. Shapiro, J. P. Simons, R. Vasudev, J. Wiesenfeld, C. Wittig, and R. N. Zare, J. Chem. Phys. **89**, 1749 (1988).
[31] B. A. Thompson, P. Harteck, and R. R. Reeves, Jr., J. Geophys. Res. **68**, 6431 (1963).
[32] K. D. Tabor and J. J. Valentini (unpublished).
[33] H. Guo and J. N. Murrell, Mol. Phys. **65**, 821 (1988).
[34] R. Schinke, R. L. Vander Wal, J. L. Scott, and F. F. Crim, J. Chem. Phys. **94**, 283 (1991).
[35] H. B. Levene and J. J. Valentini, J. Chem. Phys. **87**, 2594 (1987).
[36] T. Oka, in *Molecules in the Galactic Environment*, edited by M. A. Gordon and L. E. Snyder (Wiley-Interscience, New York, 1973), p. 257.